Morphological Consequences of Interchange Reactions during Solid State Polymerization in Oriented Polymers

Celine Almonacil, Prashant Desai, and A. S. Abhiraman*

Schools of Chemical Engineering and Textile & Fiber Engineering, Polymer Education and Research Center, Georgia Institute of Technology, Atlanta, Georgia 30332-0100

Received December 6, 1999; Revised Manuscript Received December 21, 2000

ABSTRACT: Interchange reactions during solid-state polymerization (SSP) can cause significant morphological changes in the intercrystalline regions. A coarse-grained model has been formulated for the effect of these reactions on the topological distribution of chains in the intercrystalline regions of oriented polymer morphologies. It includes a novel thermodynamic scheme, coupled with a Monte Carlo simulation, based on rotational isomeric states, of confined chains to determine the relative probabilities of topologically different reaction outcomes. The results show the role of intrinsic molecular rigidity on interchange-reaction dictated interconversions of bridges and loops during SSP of different polymers. The scheme presented here can serve to identify, via *gedanken* experiments, appropriate semirigid polymers for synthesis and processing to produce morphologies for high mechanical performance. It can also be used to determine the above-T_g mechanical properties of noncrystalline domains, with a known initial topological distribution of chains, as well as the equilibrium distribution of these chains.

Introduction

The physical properties of a semicrystalline polymer are dictated to a significant extent by the morphology of the noncrystalline phase. Four types of topological chains can exist in this phase: (i) bridges, whose ends are anchored in different crystallites, (ii) loops, whose ends are anchored in the same crystallite, (iii) anchor chains, with one end anchored in a crystallite and the other unattached, and (iv) free chains, with both ends unattached. The bridges (or tie chains) are the principal load-bearing elements[1] and thus play a critical role in determining the mechanical properties of the material.

There have been a few attempts to experimentally quantify the different topological chains in the noncrystalline regions of oriented polymers.[2,3] There is also abundant theoretical work on the thermodynamic equilibrium in semicrystalline structures. These have used free energy minimization,[1,4−8] or the Gambler's ruin approach, with either a random walk model[9−11] or an RIS scheme.[9] Varyukhin and Zaitsev have used an RIS scheme to simulate polyethylene, poly(tetrafluoroethylene), polyoxymethylene, and poly(ethylene oxide) on a diamond-type lattice, with allowance for the statistical weights of the possible conformations.[4] They have formulated a description of the amorphous region, based on partition functions that are obtained by generating bridges that span, and are confined by, two walls.[5]

Yoon has developed a theory for the strength of wholly aromatic polyesters that is based on the structure of the noncrystalline regions.[12] With data on nylon 6, obtained from NMR and IR spectroscopy, and a description of the molecular morphology that is based on the distribution of tie chains, Yegorov et al.[13,14] have also proposed a theoretical expression for the stress−strain relationship in oriented polymers.

We have shown recently that, unless limited by diffusion of the condensation molecule, the kinetics and mechanism of solid-state polymerization (SSP) in polyesters and polyamides are governed by interchange reactions.[15] An important potential morphological consequence in this regard arises from the interchange-reaction induced changes in the relative concentrations of the different topological components of the noncrystalline phase. For example, as shown in Figure 1, an anchor chain can react with a bridging chain to form either a (substitute) bridging chain or a loop. The latter would be, in most instances, ineffective as a link for stress transfer between crystals. It has to be noted that interchange reaction between an anchor chain end and a bridge or a loop can have several issues and, therefore, different morphological consequences.

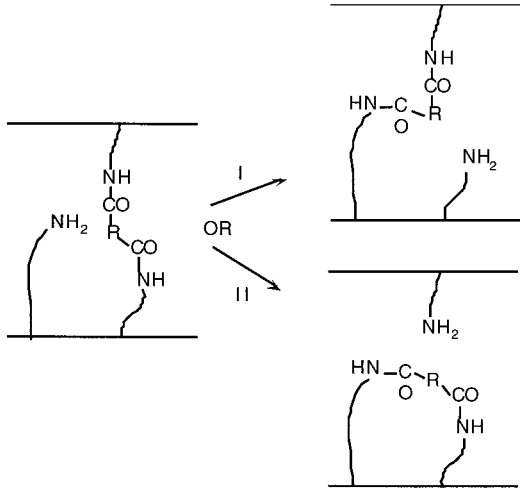

Figure 1. Example of different morphological consequences of an interchange reaction. Interchange reaction between an amine group on the anchor chain and one of the two amide groups shown here on the bridging chain can lead to the formation of another bridge and an anchor chain (I) or a loop and an anchor chain (II).

In post-extrusion solid-state polymerization, where a high extent of interchange reactions occurs, it is especially critical to determine, or at least infer, the effects of these reactions on the morphology of the polymer. If

* To whom correspondence should be addressed.

10.1021/ma9920339 CCC: $20.00
Published on Web 05/11/2001

the concentrations of topologically different chains in the intercrystalline regions can be quantified, it can facilitate the design of polymers and precursor morphologies to achieve desired properties *as a consequence of the interchange reactions*. This field of investigation has been largely neglected, although it has been recognized to have the potential to offer "new prospects in polymer physics and chemistry."[16]

Wunderlich and Miyagi have recognized that evolution of morphology during heat treatment could occur through chemically reactive crystal lamellar surfaces.[17,18] They also conclude that, through chemical reorganizations, chain folds and chain ends can be converted into tie (bridging) chains, with a consequent increase in the total number of tie chains during heat treatment of PET. They even suggest the existence of a pseudoequilibrium of tie molecules, independent of the origin of the starting material.[18]

It is well-known that SSP in *rigid* polymers can lead to a substantial increase in the tensile strength, by as much as a factor of 4. This increase in strength upon SSP of rodlike polymers has been attributed primarily to an increase in the number of bridging chains that can result directly from the increase in molecular weight.[12] It should be recognized, however, that preferential reactions of stressed chains to produce relatively stress-free chains can also have a significant effect in this regard.

There is no satisfactory theory in the current literature to predict, or even infer, the effect of reactions during SSP on mechanical properties of flexible and semirigid polymers. Kyotsukuri and Tada have reported a decrease in mechanical properties as a result of SSP of commercial nylon 66 fibers at lower temperatures, and no change at higher SSP temperatures.[19] Srinivasan et al. have reported only a small improvement in mechanical properties on post-extrusion SSP and drawing of nylon 66, despite a 7-fold increase in molecular weight.[16] Narayan et al. also report no improvement in mechanical properties of nylon 46, despite a 3-fold increase in molecular weight.[20]

Srinivasan et al. have noted that the morphology of flexible polymers could be adversely affected by the interchange reactions during SSP.[16] As a first step toward understanding this phenomenon, they have formulated a simplified kinetics-based morphological model and demonstrated a consequent evolution in the relative concentrations of the four types of topological chains.[16] This model shows how the mechanism that facilitates SSP could also cause significant changes in the concentrations of topologically different chains in the intercrystalline domains. However, the oversimplifying assumptions in the basis of this model, especially the assumption that the primary structure, topology, or length of a chain does not influence the relative rates of interchange reactions at different sites, precluded quantitatively valid predictions of the evolution of morphology through their analysis. These issues constitute the primary focus of the present study.

The possible locations of the functional groups and the morphological consequences of their interchange reactions during SSP of polyamides are listed in Table 1. The acid−amide and amide−amide reactions have been assumed to be negligible in comparison to amine−amide interchange reactions. For polyesters, if the alcohol−ester is considered to be the only interchange reaction, a similar table is obtained, with the amine group in polyamides replaced by the hydroxyl group and the amide link by the ester link.

Table 1. Morphological Consequences of Amine−Amide Interchange Reactions during Solid State Polymerization of Polyamides, as a Function of the Locations of the Functional Groups

	location	
functional group	amine/anchor chain (AC)	amine/free chain (FC)
amide/loop	loop + AC or bridge + AC	AC + AC
amide/bridge	loop + AC or bridge + AC	AC + AC
amide/anchor chain	loop + FC or bridge + FC	AC + FC
amide/free chain	AC + FC	FC + FC

It is important to be cognizant of the fact that the reactions listed in Table 1 would have different probabilities, or relative rates, of occurrence. The probability of a given reaction will be dictated by the types (such as loops and bridges), as well as the lengths, of the topological chains reacted, and produced, in these reactions. Also, the intrinsic rigidity of a chain would dictate its preferential existence as a loop or a bridge in an intercrystalline region; i.e., *relative thermodynamic preferences for the formation of different topological chains would be dictated by the intrinsic rigidity of the polymer*. Thus, to quantify the effect of interchange reactions on molecular-level morphology, it is necessary to develop a scheme to determine the probabilities of topologically different reaction pathways.

The work reported here constitutes the formulation of a thermodynamic framework to determine the relative probabilities of different morphological outcomes of interchange reactions, with due consideration of the primary structural features of specific polymers. This framework has been incorporated into a Monte Carlo scheme, with a coarse-grained reaction model, to determine the evolution of morphology in intercrystalline domains during SSP of *oriented* polymers. Broader implications of the new approach have also been explored, especially with regard to equilibrium structures and mechanical properties of the noncrystalline domains in semicrystalline polymers, at temperatures well above their glass transition.

System Description

The system considered in this work represents an intercrystalline domain in an oriented semicrystalline polymer with high uniaxial crystalline orientation. It consists of the set of chains that emanate from opposite faces of two crystals. The area of each face is taken to be $(50\ \text{Å})^2$, with 100 chains emanating from each face. Intercrystalline wall distances of 30, 50, 70, 100, and 120 Å have been considered in this work. The polymers considered in this regard, polyesters and polyamides, are known for their propensity to undergo interchange reactions during SSP.

The following assumptions and approximations have been used in the model.

1. The constraint imposed on the intercrystalline chains by the impenetrable crystal boundaries has been represented by two parallel impenetrable surfaces of infinite extent.

2. A molecular modeling scheme has been used to determine the partition functions of chains in an intercrystalline region, as functions of their contour length (the number of repeat units) and topological classification (loop, anchor chain, or bridge). A simulated chain of chosen contour length that emanates from a crystal

Table 2. Possible Morphological Reorganizations upon Interchange Reaction in the System Studied[a]

chain A	chain B	chain A′	chain B′
top AC	bottom loop	bridge	top AC
bottom AC	top loop	bridge	bottom AC
top AC	top loop	top loop	top AC
bottom AC	bottom loop	bottom loop	bottom AC
top AC	bridge	top loop or bridge	bottom AC or top AC
bottom AC	bridge	bottom loop or bridge	top AC or bottom AC

[a]Functional end group on chain A reacts with a functional linkage on chain B to form two (substitute) chains, A′ and B′. AC denotes anchor chains

face is considered to be a bridge if the other end terminates within a short distance, δ, of the opposite face, a loop if it lies within δ of the emanating face, and an anchor chain otherwise. This aspect will be addressed further in a later section.

3. Only the interchange reaction between an end group and a reactive linkage is considered. This is equivalent to considering only the amine−amide interchange in polyamides, or the alcohol−ester interchange in polyesters, each of which is known to be the dominant interchange reaction in their respective systems. Other possible interchange reactions, such as acid−amide, amide−amide, and ester−ester, are not considered. However, it should be recognized that incorporation of these other reactions is necessary only if a *real time kinetic analysis* of evolution of morphology is to be carried out. Their inclusion would not change the asymptotic equilibrium distribution of chains.

4. There are initially no free chains in the system. The high initial molecular weights that are typical in solid-state polymerization make this a reasonable assumption. The very low end group concentration renders the probability of existence of free chains negligible in relation to other chains.

5. The system contains only one anchor chain; i.e., no polymerization occurs. This assumption has been used in order to focus the analysis on the topological consequences of interchange reactions, without introducing the unnecessary complexities that would arise due to the different rates of polymerization and interchange reactions.

6. The topological chains (loops, bridges) consist of complete repeat units. Restricting the system to chains of multiple repeat units simplifies the computations, but does not reduce the generality of the results. Also, for ease of tracking of chain compositions, the anchor chain is constituted to have an additional monomer unit, with an amine functional group at its end.

7. Intrachain interchange reactions are neglected.

Assumptions 4, 5, and 7 imply, together, that no free chains are ever present in this system, so that the only topological units that can exist in the system are loops, bridges, and an anchor chain. The morphological reorganizations that can occur under these conditions are listed in Table 2.

To quantitatively model the effect of intrinsic rigidity, several semiflexible polymers with rigid moieties (such as *p*-phenylene, naphthalene, and anthracene), and flexible moieties (methylene units, for example) have been studied. The polymers analyzed in this work are shown in Figure 2. Among these, poly(ethylene terephthalate) (PET), poly(butylene terephthalate) (PBT), and nylon 66 are industrially important polymers, each produced in large volume. Poly(ethylene naphthalate) (PEN) is under consideration for many applications.[21] Poly(butylene naphthalate) (PBN) has been the subject of several studies.[22−24] Nylon 2T, 4T, and 6T have been previously synthesized.[25,26] A polymer that is close to polyethylene anthracate (PEA) has been synthesized previously.[27] Poly(butylene bibenzoate) (PBBB) and other polymers similar to polyethylene bibenzoate (PEBB), but with three to six methylene units, have been synthesized.[28,29] Poly(butylene anthracate) (PBA) will also be considered in this study. A copolyester of 2,6-dimethyl naphthalate and dimethyl-4,4′-bibenzoate (PENBB) has been formed into films.[30]

In each polymer, the number of sites available for interchange reaction is equal to $2nl_{av}$, where n is the number of chains in the system, and l_{av} is the average number of repeat units per chain. The appropriate l_{av} of each polymer was obtained as the nearest integer to

$$l_{av} \approx \frac{\rho \bar{h} (50 \times 10^{-10})^2 N_A}{n m_{RU}} \quad (1)$$

where ρ is the density of the intercrystalline domains (in kg/mol), $\bar{h}$ is the intercrystalline wall distance (in m), m_{RU} is the molar mass of a repeat unit (in kg/mol), and N_A is Avogrado's number, so that l_{av} is expressed in number of repeat units.

The densities of the intercrystalline domains in many of these polymers are not known. The crystalline density is used in its place, with the assumption that the noncrystalline densities in the oriented morphologies of these polymers would be correlated with the crystalline densities. For polymers with unreported densities, they were estimated using the QSPR module of the Insight II software, which uses the group contribution methodology of Van Krevelen.[12] The density used for each polymer is listed in Table 3. The average number of repeat units per segment for each of the intercrystalline wall distances considered in this work is reported in Table 4.

Methodology

The typical size of an intercrystalline domain in an oriented semicrystalline polymer is of the order of (50 Å)^3, with approximately 40 000 atoms. Atomistic simulations of reactions in polymeric systems of these sizes are not yet practical. Therefore, coarse-grained approaches are commonly used.[31] The typical amorphous domain in a semicrystalline material contains up to 10^3 linkages for exchange reactions. A stochastic method, such as the Monte Carlo simulation technique, is well suited to study reactions in such systems.

Monte Carlo simulation techniques have been shown to be useful to model interchange reactions. Montando formulated a non-space-filling approach to study the effect of the exchange reactions on a copolymer's composition.[32] Using this approach, he concluded that an "end group−ester" interchange (either alcohol−ester or acid−ester interchange) is in better agreement with experimental data on polymerization of copolyesters than ester−ester interchange. Jo et al. used a Monte Carlo technique to simulate the effect of interchange reactions on the molecular weight distribution of PET.[33] Their results showed that the system quickly evolved to the most probable molecular weight distribution. Jang et al. also simulated interchange reactions in polyester blends using a simple cubic lattice.[34]

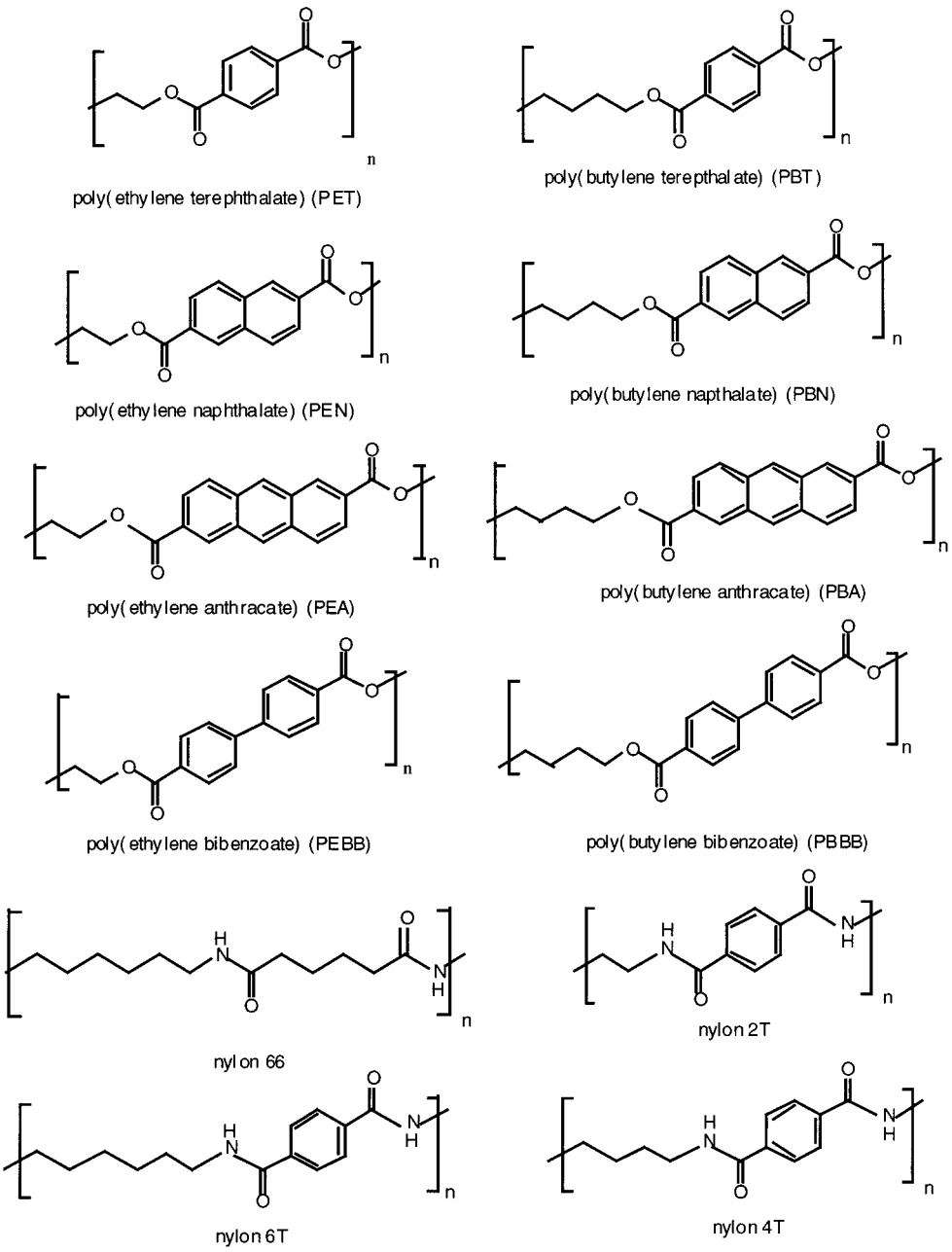

Figure 2. Polymers modeled in this study.

Table 3. Densities Used for Calculation of Average Number of Repeat Units Per Chain and Extended Length of a Single Repeat Unit of the Different Polymers Modeled in This Work

polymer	density (kg/m^3)	extended repeat (Å)
PET	1450	10.75
PEN	1400	13.20
PEA	1350	15.65
PEBB	1360	11.88
PBT	1340	13.24
PBN	1320	15.06
PBBB	1310	13.74
PBA	1300	17.22
nylon66	1160	17.20
nylon 6T	1210	15.60
nylon 4T	1250	13.16
nylon 2T	1310	10.63

Table 4. Average Number of Repeat Units per Chain at Different Intercrystalline Wall Distances for the Polymers in This Study

	wall distance (Å)				
polymer	30	50	70	100	120
PET	4	6	8	12	14
PEN	3	4	6	9	11
PEA	2	3	5	7	8
PEBB	3	4	5	8	9
PBT	6	10	12	18	22
PBN	4	8	10	14	18
PBA	4	6	8	12	14
PBBB	4	6	10	14	16
66	3	4	6	8	10
6T	2	4	5	7	9
4T	3	4	6	9	10
2T	3	5	7	10	12

Reaction Scheme. The possible morphological reorganizations that can occur, when an anchor chain A of length l_A reacts with a chain B of length l_B to form two (substitute) chains A′ (of length l'_A) and B′ (of length l'_B), are listed in Table 2. All chains are assumed to be made of symmetric repeat units, with each chain being made of a multiple number of repeat units. The coarse-

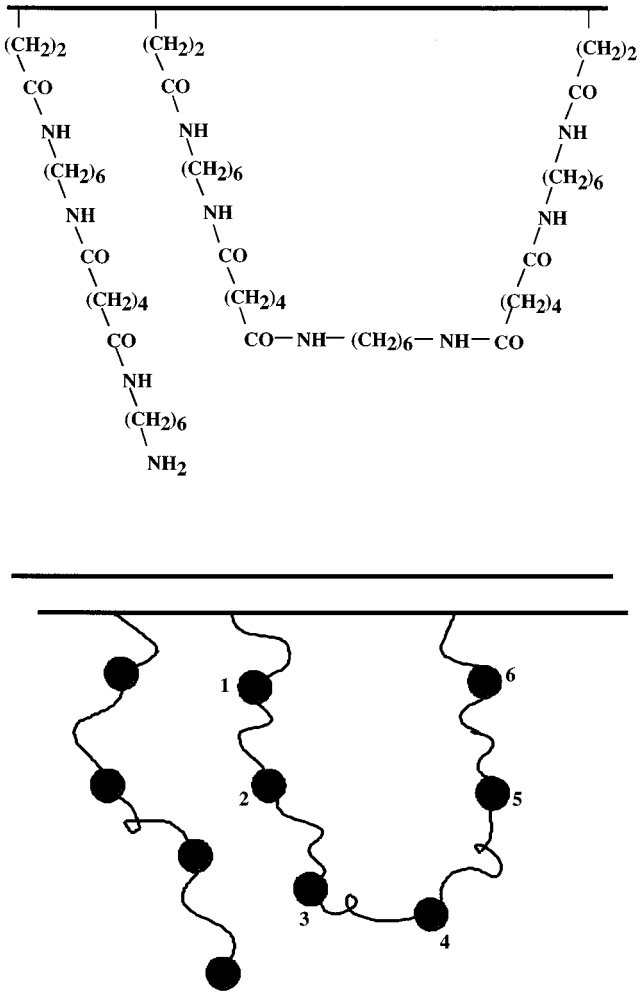

Figure 3. Example of coarse-graining procedure for nylon 66. Each amine/amide group constitutes a reactive site.

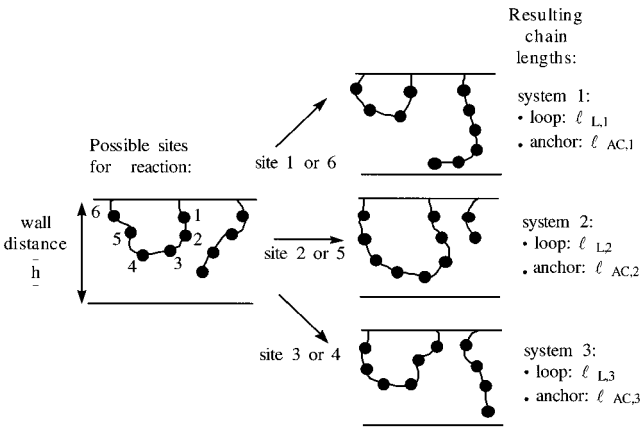

Figure 4. Example of possible reaction sites, and the consequent outcomes, for interchange reaction between a loop and an anchor chain on the same crystal face. There are six sites available for interchange reaction, with three outcomes that are distinguishable in the framework of the current model.

graining scheme that has been used to describe the functional sites for interchange reactions in chains is illustrated with nylon 66 in Figure 3.

Using such a coarse-grained description, it is possible to establish a set of rules for the possible interchange reactions. It is exemplified by considering the case shown schematically in Figure 4. Assuming that sites at the same distance from the closest wall along the polymer chain have the same probability of reaction, there would be three possible outcomes for the interchange reaction between a loop with 6 reactive sites and an anchor chain. (Note: the positions of chains *along a wall* are not to be taken literally in these schematic figures.) With every case in this illustration, the interchange reaction leads to the formation of an alternate set of loop and anchor chain. However, depending on the site of reaction, the chains formed would have different lengths. In the current model, chains of the same length within any one of the three classes of chains (anchor, loop, bridge) are assumed to be topologically indistinguishable.

Examining all the possible reactions listed in Table 2, it is possible to write a consistent scheme for all sites. This is appropriate for a system of symmetric repeat units, with all the chains made of an integral multiple of such units. With the reaction sites numbered in sequence, beginning with the site closest to the wall, the chain lengths are modified by interchange reactions according to the following rules.

If the site has an odd number, the chain lengths of A and B are obtained from

$$l'_{\mathrm{L},i} = l_{\mathrm{AC}} + (i - 1) \tag{2}$$

$$l'_{\mathrm{AC},i} = l_{\mathrm{L}} - (i - 1) \tag{3}$$

If the site has an even number, the chain lengths are obtained from

$$l'_{\mathrm{L},i} = l_{\mathrm{AC}} + l_{\mathrm{L}} - i \tag{4}$$

$$l'_{\mathrm{Ac},i} = i \tag{5}$$

where the primed quantities refer to the product chains and the unprimed quantities to the reacting chains. AC and L refer, respectively, to anchor chain and loop.

The necessary length constraints are taken into account in the probability scheme, so that no site that would lead to the formation of "forbidden" chains, e.g., bridges shorter than the wall distance, can be picked.

In a real system, an end group has the possibility of reacting with all the reactive sites that are accessible to it. Then, preferential reaction of one of the functional sites over another would be dictated by the partition functions of the different product chains. Since no space-filling issues have been considered in the current model, the following scheme has been adopted for choosing of possible sites for reaction: A chain is first picked, and then a site on this chain is chosen for reaction, with the probability of the former step weighted by the chain length and the probability of the latter dictated by the partition functions of the resulting chains. The length-dictated choice of the chain to be reacted is based on the fact that a longer chain is more likely to have a reactive group in the vicinity of a given end group than a shorter chain. This simple procedure for choosing the reacting bridge or loop at a step would not alter the dynamic equilibrium of chains that would result. However, if the progression to this equilibrium is to be modeled properly, it would have to be replaced by a computationally extensive scheme that follows the spatial coordinates of all the sites for interchange reactions.

Once the chains are chosen, a reaction site is selected according to the rules described in the following thermodynamic scheme.

Scheme for Relative Probabilities of Reaction Pathways with Topologically Different Outcomes. The procedure used to calculate the probabilities of reactions at different functional sites on a chain is illustrated by using the example given in Figure 4. In this case, the probability of reaction at site 1 (to form system 1), p_1, at site 2 (to form system 2), p_2, and at site 3 (to form system 3), p_3, have to satisfy

$$p_1 + p_2 + p_3 = 1 \tag{6}$$

The ratio p_1/p_2 is postulated to be

$$\frac{p_1}{p_2} = \frac{Q_1}{Q_2} \tag{7}$$

where Q_1 and Q_2 are the partition functions of systems 1 and 2, respectively. These partition functions are given by

$$Q_1 = Q_L\{l_{L,1},\bar{h}\}\, Q_{AC}\{l_{AC,1},\bar{h}\} \tag{8}$$

$$Q_2 = QL\{l_{L,2},\bar{h}\}\, Q_{AC}[l_{AC},2,\bar{h}\} \tag{9}$$

where $Q_L\{l_{L,1},\bar{h}\}$ is the partition function of a loop of contour length $l_{L,1}$, $Q_{AC}\{l_{AC,1},\bar{h}\}$ is the partition function of the anchor chain of contour length $l_{AC,1}$, and similarly for other chains. A similar scheme can be written for a system with N topological chains instead of just the two chains considered in this example.

Because of the spatial constraints imposed on the chains by the impenetrable crystal boundaries, one has to consider the partition function of a chain of specific contour length that is confined between walls. It can be obtained through the following technique.

The partition function of a chain, e.g., a bridge of contour length l, confined between two walls at a distance $\bar{h}$, $Q_B\{l,\bar{h}\}$, can be written as

$$Q_B\{l,\mathrm{h}\} = \frac{Q_B\{l,\bar{h}\}}{Q\{l\}}\, Q\{l\} \tag{10}$$

where $Q\{l\}$ is the partition function of an unconfined chain of contour length l. $Q\{l\}$ can be calculated using the RIS theory. The ratio of wall-constrained and unconstrained chain partition functions, $Q_B\{l,\bar{h}\}/Q\{l\}$, can be estimated using a Monte Carlo rotational isomeric state (RIS) simulation, as described in the following section.

Monte Carlo Simulation of Bridges, Loops, and Anchor Chains. The objective of the Monte Carlo simulation is to obtain an estimate of the ratio of wall-constrained and unconstrained partition functions that is required in eq 10. For example, consider the ratio, $Q_B\{l,\bar{h}\}/Q\{l\}$, which represents the ratio of partition function of a bridge of contour length, l, that spans two crystals, separated by a distance $\bar{h}$. If one constructs, through an appropriately weighted statistical scheme, a set of N chains of contour length, l, each emanating from the boundary of a crystal, then an estimate of this ratio will be provided by

$$\frac{Q_B\{l,\bar{h}\}}{Q\{l\}} = \frac{N_B\{l,\bar{h}\}}{N\{l\}} \tag{11}$$

where $N\{l\}$ is the total number of chains generated and $N_B\{l,\bar{h}\}$ is the number that satisfies the conditions that are necessary for them to be bridging chains of the *specified contour length and intercrystalline distance*.

Note: In the descriptions given above, and in those that follow, a chain refers only to the part of a complete polymer molecule that lies within an intercrystalline region. Also, the two "ends" of a chain in this regard refer to the ends of the intercrystalline part of a polymer molecule and not to the two ends of the whole polymer molecule.

The Monte Carlo rotational isomeric state (RIS) method[35] allows, through stochastic simulations, the generation of polymer chains that are representative of the relative populations of loops, bridges, and anchor chains. The RIS scheme is particularly suitable for this purpose, since it allows modeling of polymers of different primary structures, while keeping the computational cost at a minimum.[36] The rotational isomeric states have been limited to those that correspond to minima in internal energy.

The required statistical weights for a variety of polymers can be found in the literature. In this study, the statistical weights for nylon 66 and PET have been obtained from Flory's work.[37,38] The statistical weights for PEN, PEA, and PEBB have been taken to be similar to those for PET, but with the bond lengths and angles adjusted to take into account the different ring structures. The statistical weights for PBT have been given by Bahar and Mattice.[39] The statistical weights for PBN, PBBB and PBA have been assumed to be similar to those for PBT. The statistical weights for nylon 6T, 4T and 2T have been obtained from those for nylon 66, considering the benzene ring as a trans double bond, following accepted procedures.[40]

The constraints due to crystal walls have been taken into account in the following way. Each chain is considered to start at a wall ($x = 0$), with the previous bonds of the chain in the crystal and the crystal c-axis perpendicular to the wall. To account for the constraints that could arise from all the other chains that also emanate from the same crystal face, the first three bonds of the modeled chain are restricted to be in the same conformational sequence as that in the crystal.

Chain Classification. A total number N_T of chains ($N_T = 100\,000$) are generated. As each chain is generated, the position of its "growing" end along the x-axis is monitored. If chain the backbone of a chain should cross either wall *prematurely*, i.e., if a chain should cross the wall, either at $x = 0$ or $x = \bar{h}$, before its full contour length has been constructed, then is considered a "rejected" chain. Such chains could not qualify as a bridge, loop or anchor chain of the *specified* contour length.

Ideally, if an "accepted" chain that emanates from a wall is such that its other end terminates at exactly the opposite wall, then it would correspond precisely to a bridging chain. One can define similarly the exact requirement for a chain to be a loop. However, to obtain the required estimates within a reasonable number of trails (chains constructed) in a simulation scheme, such exact requirements have to be relaxed. Also, in a Monte Carlo scheme that restricts the spatial paths of the chains to those that are *dictated by a discrete set of backbone bond conformations*, imposing an exact condition on the ends would artificially make the fraction of bridges and loops negligible and thus lead to incorrect results. It is due to this reason that a simulated chain of a specific contour length that emanates from a crystal

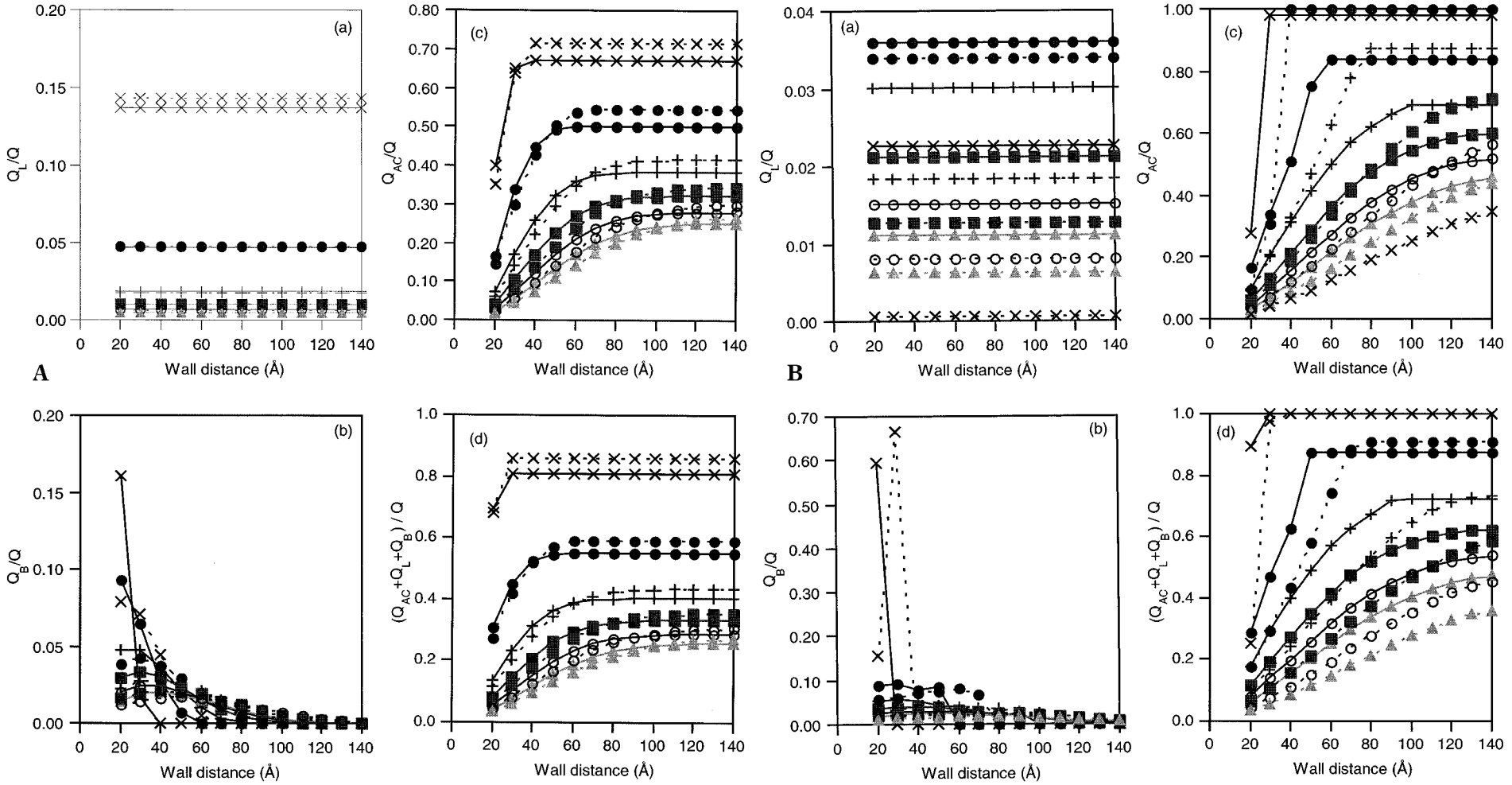

Figure 5. (A) Partition function ratio of topological chains of different chain contour lengths, as a function of intercrystalline wall distance, calculated using Monte Carlo RIS approach: (a) loops, (b) bridges, (c) anchor chains, and (d) accepted fraction of "loops + bridges + anchor chains." Key: full lines, nylon 66; dotted lines, nylon 6T. Chain lengths: (×) DP = 2, (●) DP = 5, (+) DP = 10, (■) DP = 15, (○) DP = 20, (▲) and DP = 25. (B) Same as part A, *except*: full lines, PET; dotted lines, PEA.

surface, and *does not penetrate either wall prematurely* along its path, is considered to be a bridge or loop if it terminates within a short distance, δ, of the corresponding wall. All the other "accepted" chains are taken to be anchor chains. To produce reasonable acceptance rates, the distance δ has been taken as 5 Å. The smallest acceptance rate, obtained with $\delta = 5$ Å, was 3.3%.

For each wall distance and each contour chain length, the numbers of loops (N_L), bridges (N_B) and anchor chains (N_{AC}) are recorded.

Partition Function Ratios. The numbers of loops, bridges, and anchor chains are used to calculate the required partition function ratios for different topological chains. At a given wall distance, $\bar{h}$, and chain length, l, the partition function ratios for the three classes of chains (eq 10) are obtained from eq 11 and the following eqs 12 and 13.

$$\frac{Q_L\{l,\bar{h}\}}{Q\{l\}} = \frac{N_L\{l,\bar{h}\}}{N\{l\}} \tag{12}$$

$$\frac{Q_{AC}\{l,\bar{h}\}}{Q\{l\}} = \frac{N_{AC}\{l,\bar{h}\}}{N\{l\}} \tag{13}$$

where $N\{l\}$ is the total number of chains generated (accepted and rejected) ($N\{l\} = N_T$), and $Q_B\{l,\bar{h}\}$, $Q_L\{l,\bar{h}\}$, and $Q_{AC}\{l,\bar{h}\}$ are, respectively, the partition function of a bridge, a loop, and an anchor chain of length l confined between two walls at a distance $\bar{h}$. For each polymer, the simulations have been carried out for each of seven different chain lengths, as specified by the number of repeat units (1, 2, 5, 10, 15, 20, and 25). The extended lengths of repeat units of the different polymers are given in Table 3.

Figure 5 shows the results of the MC−RIS simulations for nylon 66, nylon 6T, PET, and PEA. The results for other polymers have been given by Almonacil.[42] These results show that the partition functions of different topological chains, especially bridges and anchor chains, are strong functions of both the intercrystalline wall distance and chain length. The polymer's intrinsic rigidity also strongly affects the partition functions of different topological chains.

Results and Discussion

The results presented in the following section represent, in each case, averages of 10 simulation runs.

Topological Composition: Bridges and Loops. Figure 6 shows the effect of interchange reactions on the bridge content for two different *starting* morphologies, one with only bridges and the other with only loops (all chains being initially of the same length) for an intercrystalline wall distance of 50 Å. Robustness of the simulation procedure is well demonstrated by the fact that the same dynamic equilibrium in topological composition is reached when starting with these two vastly different morphologies.

The equilibrium bridge content is expected to increase with increasing intrinsic rigidity. This is indeed observed for the polyesters, PBT, PET, PEN, and PEA, as shown in Figure 7a. The results for PEBB, PBN, PBBB, and PBA are shown in Figure 7b. As expected, the bridge content at equilibrium for PEN is higher than that for PBN. From these results, the bridge-forming tendency of PEBB seems to fall between that of PEN and PEA. PBN, PBBB, and PBA do not appear to have a significantly higher bridge-forming potential than

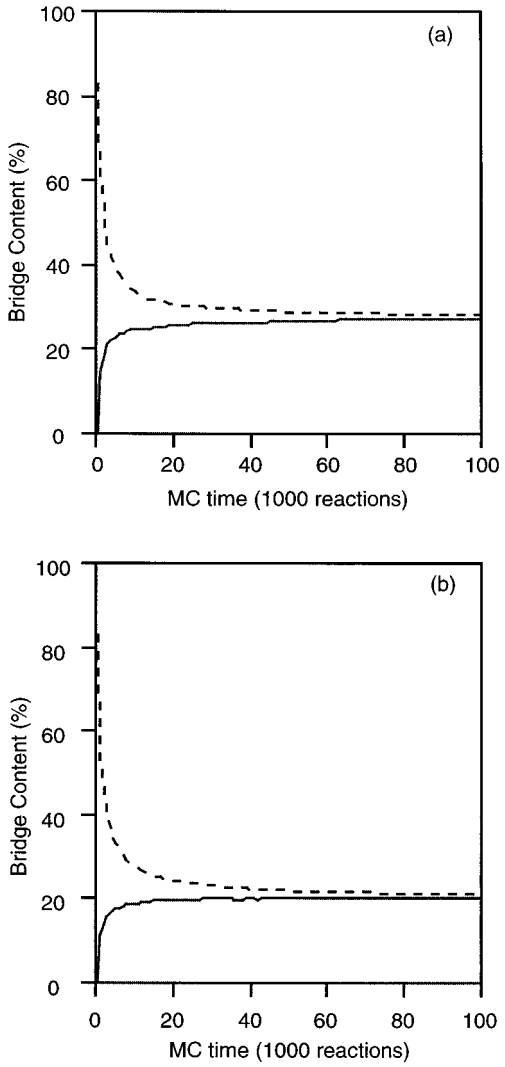

Figure 6. Evolution of the bridge content during SSP for different initial morphologies, at an intercrystalline wall distance of 50 Å (1MC time = 1000 interchange reactions, running averages, averaged over 10 simulation runs). Full lines: initially no bridges. Dashed lines: initially no loops. Key: (a) PET; (b) Nylon 66.

PBT. Although the equilibrium bridge content does increase with incorporation of intrinsically more rigid moieties in these in these polyesters, the results show clearly that a thermodynamically driven higher performance morphology, i.e., one with a high fraction of intercrystalline bridging chains, does not evolve until a high degree of intrinsic rigidity is designed into the primary backbone structure. These results are further corroborated by the computations with polyamides (Figure 7c). While computations on a finer scale in the division of chain lengths and rotational isomeric states, with more rigorously verified statistical weights, might serve to order these polymers more accurately with regard to their bridge-forming potential, it should be noted that the equilibrium bridge concentrations of all the four polyamides in this series are too low to be of interest in seeking thermodynamically driven higher performance morphologies.

For the polymers considered in this study, the portion of tie chains at equilibrium ranges from 16% to 70% for a wall distance of 50 Å, the typical intercrystalline spacing in oriented semicrystalline polymers. The lower end of these results, 16%, compares well with the results

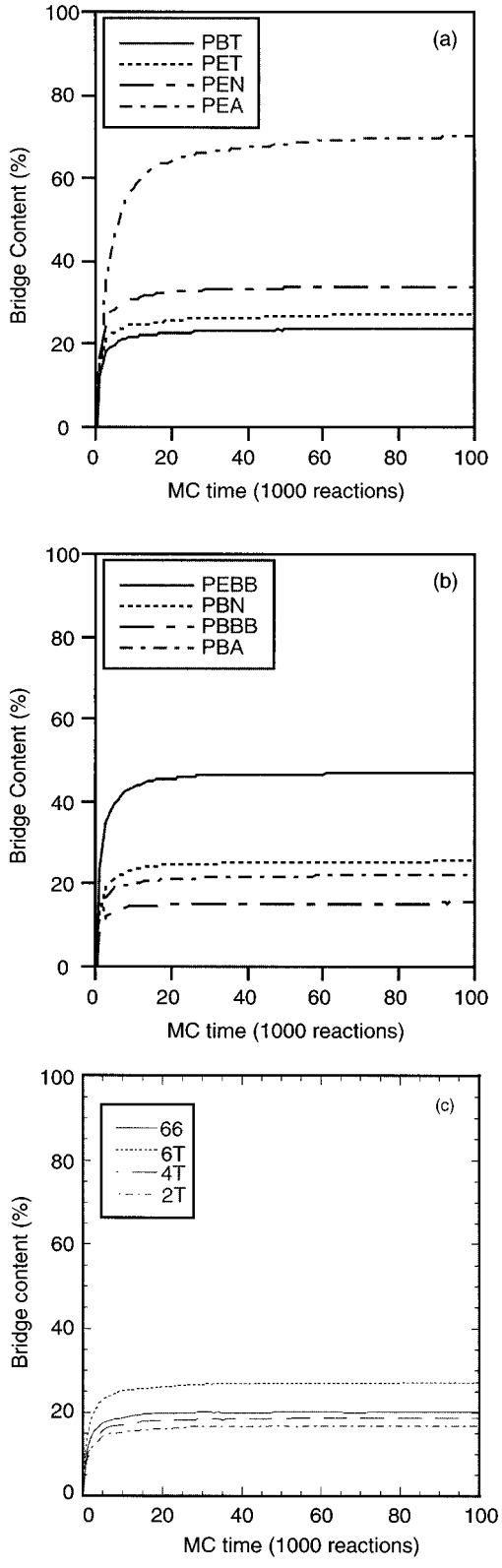

Figure 7. Evolution of the bridge content during post-extrusion SSP of different polymers from a system with initially no bridges and an intercrystalline wall distance of 50 Å (1MC time = 1000 interchange reactions, running averages, averaged over 10 simulations runs): (a and b) polyesters; (c) polyamides.

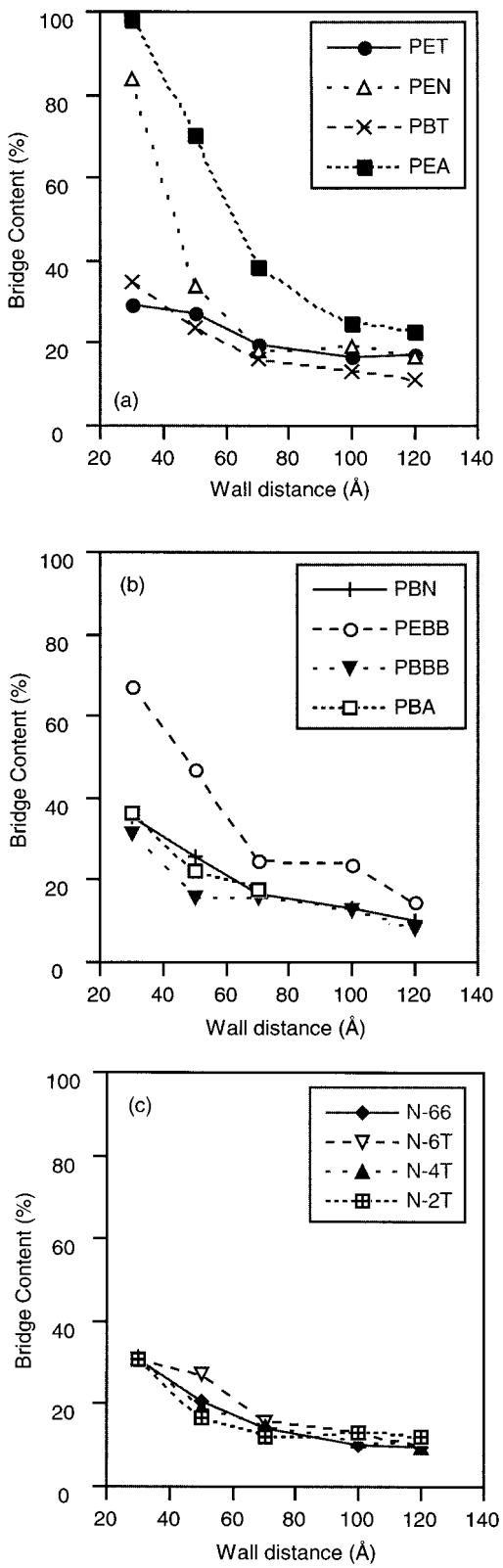

Figure 8. Equilibrium bridge content, as a function of intercrystalline wall distance, for various polymers (system after 100 000 interchange reactions from an *initial system with no bridges*, averaged over 10 simulation runs).

of Zaitsev and Varyukhin's simulations of polyethylene on a diamond-type lattice, which yields a tie chain content of 15% at an intercrystalline distance of 50 Å.[4,5]

These results have profound implications regarding the evolution of morphology during post-extrusion SSP. Depending on whether the precursor (pre-SSP) morphology has a lower or higher intercrystalline bridge content than the thermodynamic equilibrium, interchange reactions during SSP treatment would tend to increase or decrease the bridge content. In a precursor with a high bridge content, its decrease during SSP

treatment can be especially rapid in the initial stages.

The structure of drawn fibers and films is most likely to be far from that corresponding to thermodynamic equilibrium. It is important to realize that, during SSP of these materials, the evolution of morphology due to interchange reactions would occur concurrently with the increase in molecular weight. The morphological changes caused by the interchange and polymerization reactions can act together, or compete, to either enhance or diminish their mechanical properties. With many of the semiflexible polymers considered in this work, the bridge content of the precursor is likely to be significantly higher than the bridge content at thermodynamic equilibrium, especially if the precursor is drawn prior to SSP. In such cases, interchange reactions during post-extrusion SSP would tend to produce a substantial decrease in bridging chains.

Figure 8 shows the equilibrium bridge content for different intercrystalline wall distances. The smooth curves presented in Figure 8 show that averaging over 10 simulations removes most of the noise in the results. For all these simulations, the number of sites at a given wall distance has been determined from eq 1, so that the average normalized length is independent of the wall distance. The equilibrium bridge content should decrease with increasing wall distance, as was also inferred by Zaitsev and Varyukhin for polyethylene.[5] The decrease in bridge content is especially significant with the relatively more rigid polymers.

As expected, the bridge content of all the polymers approaches the "flexible polymer limit" at large intercrystalline wall distances (intercrystalline spacing). These calculations show clearly that, to take advantage of the bridge-forming potential of more rigid linear polymers, it is also essential to process them so that a high level of crystallinity and a *high frequency of crystallization* (i.e., high primary nucleation rate) are obtained. It is best exemplified by the fact that, with the different polymers modeled here, the equilibrium bridge content ranges from 0% to 98% for an intercrystalline wall distance of 30 Å, while it ranges from 8% to a high of only 22.5% at 120 Å. These results are in agreement with the inferences of Guttman, DiMarzio, and Hoffman, "the thicker the amorphous phase the weaker is the material".[41]

Distribution of Intercrystalline Chain Lengths. The framework developed in this work can provide not only information regarding evolution in the concentrations of different topological chains but also the probability distribution of chain lengths within each topological component. These distributions can be obtained from

$$P_B(\bar{l}_i) = \frac{n_B(\bar{l}_i)}{\sum_i n_B(\bar{l}_i)} \tag{14}$$

$$P_L(\bar{l}_i) = \frac{n_L(\bar{l}_i)}{\sum_i n_L(\bar{l}_i)} \tag{15}$$

where $n_B(\bar{l}_i)$ and $n_L(\bar{l}_i)$ correspond, respectively, to the number of bridges and loops of "normalized" length $\bar{l}_i$ in a given system. To allow for more meaningful interpretations, these distributions have been calculated

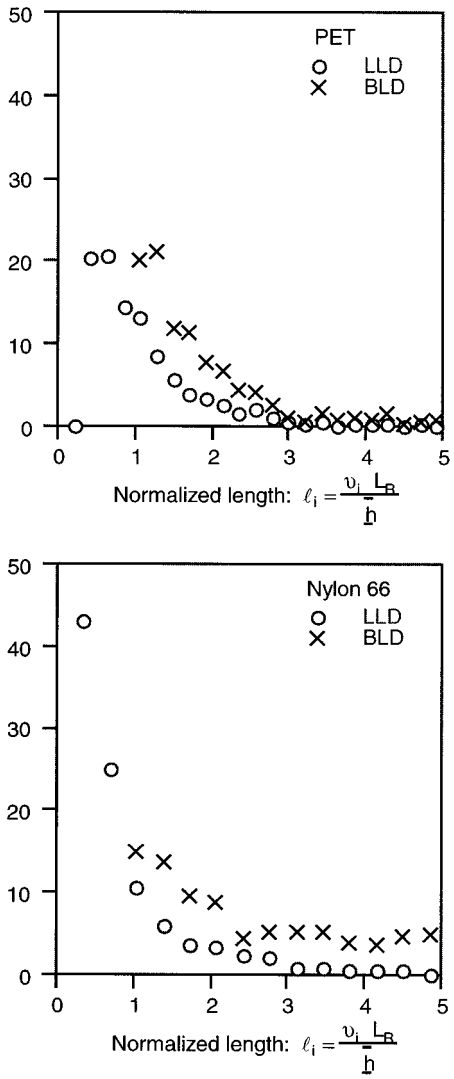

Figure 9. Probability distribution (%) of lengths of loops (LLD) and bridges (BLD) after 100 000 interchange reactions from an *initial system with no bridges*; intercrystalline distance = 50 Å. The distributions were obtained from averages over 10 simulation runs. (l_i = contour length of a bridge with v_i repeat units; L_R = extended length of a repeat unit; $\bar{h}$ = intercrystalline wall spacing).

using the normalized chain length

$$\bar{l}_i = \frac{v_i L_R}{\bar{h}} \tag{16}$$

where L_R is the extended length of a repeat unit and v is the degree of polymerization of the chain.

Figure 9 shows the distribution of chain lengths after 100 000 interchange reactions in a system initially with only loops, while Figure 10 shows the distribution of chain lengths obtained from a system initially with only bridges. In both cases, all the chains were initially of the same length. As can be seen by comparing Figures 9 and 10, similar distributions have been obtained from the two completely different initial morphologies, suggesting that the number of reactions run is sufficient to reach dynamic equilibrium. The distributions for other polymers, PEN, PEBB, PBT, PBN, PBBB, nylon 66, nylon 2T, nylon 4T, and nylon 6T, have also been computed, and these can be found in ref 42.

The distributions of chain lengths in flexible semicrystalline polymers have been obtained by Zaitsev and

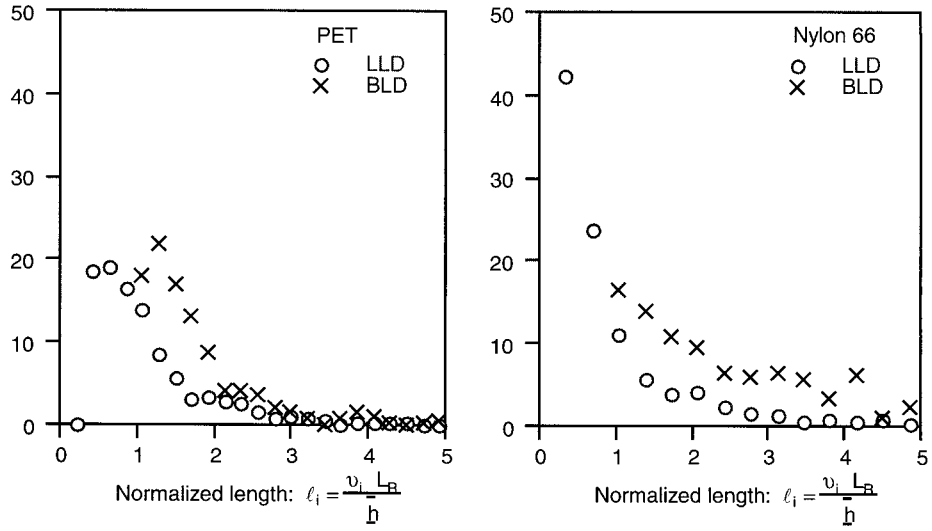

Figure 10. Same as Figure 9, except for an *initial system with no loops.*

Varyukhin[4,5] from statistical mechanical simulations, and by Leermakers et al.[10] from Gambler's ruin analysis. Their distributions are qualitatively similar to the results obtained in this work. Leermakers et al.[10] found that, for a flexible polymer, the number of loops of a given length decreases with increasing chain length, but it exhibits a maximum for stiff chains. According to these results, which are also in agreement with those of Zaitsev and Varyukhin,[5] nylon 66 would correspond to a flexible chain and the other polymers would correspond to relatively stiffer chains. Zaitsev and Varyukhin showed distributions of bridge lengths with broad tails for undrawn polymers,[5] similar to those obtained in this work. However, Popli and Roylance, using the method of images, obtained distributions of bridge lengths that did not exhibit such broad tails.[1]

The distributions of chain lengths would play a significant role in determining the mechanical properties of the material. The optimum distribution will depend on the combination of properties desired in the material. In general, the strength should increase with increasing bridge content, and decrease with increasing breadth of the distribution of bridge chain length. The strain to failure will increase with the fraction of noncrystalline phase and average length of bridging chains, normalized by the intercrystalline distance $\underline{\bar{h}}$. Obviously, higher stiffness would result from higher crystalline fraction in the material and also from shorter bridging chains. If an application requires a high recoverable work, it would be desirable to produce a narrow distribution of bridging chain lengths, with a high average normalized length. On the other hand, if dissipation during deformation to failure is desirable, an appropriately broad distribution can produce it through sequential scission of bridging chains during the deformation process.

Guttman, DiMarzio, and Hoffman have inferred that the extensibility of a polymeric material should increase with increasing intercrystalline distance.[41] The material's extensibility in this regard would be dictated by the combined influence of the extent of the noncrystalline phase and its extensibility. The average normalized bridge length decreases with increasing polymer rigidity (Figure 11). In almost every case, it increases and then appears to go through a weak maximum as a function of wall distance. In general, the computed average of normalized bridge length suggests that these polymers do yield a more extensible equilibrium noncrystalline domain structure at higher wall distances.

Equilibrium Stress−Strain Relations. The confined-chain partition functions, obtained as functions of contour lengths and wall distances, can also be used to establish the equilibrium, above-T_g, stress−strain relationships of noncrystalline domains, with a known topological composition in the undeformed state. If $\{Q_i(l_i, \underline{\bar{h}})\}$ represents the complete set of partition functions of the chains in a noncrystalline domain, with its crystalline boundaries at a distance, $\underline{\bar{h}}$, apart, then the free energy of this set of chains, $G\{\underline{\bar{h}}\}$, is given by

$$G\{\underline{\bar{h}}\} = \sum_i -kT \ln Q_i(l_i, \underline{\bar{h}})$$

and the force−extension relationship for this domain is given by

$$f\{\underline{\bar{h}}\} = \frac{\partial G}{\partial \underline{\bar{h}}}$$

Almonacil has demonstrated that the procedure can be followed to predict the stress−strain relationship, taking oriented semicrystalline poly(ethylene terephthalate) as an example.[42] However, larger scale simulations, with a much finer sequence of wall separations and division of chain conformational states, have to be carried out before reliable stress−strain relations can be computed.

Other Issues. The calculations performed in this study were carried out using the statistical weights that have been reported at 25 °C. It should be noted that, to determine precisely the consequences of interchange reactions during SSP of a polymer, these have to be performed *at the SSP temperature.* An obvious way in which it would change the results of the present analysis is to reduce further the reported bridging chain concentrations. The implication is that primary polymer structures with even higher rigidity than those identified through the present study would be necessary to achieve thermodynamically dictated high performance morphologies.

Because of current computational limitations, the framework used here does not consider spatial packing

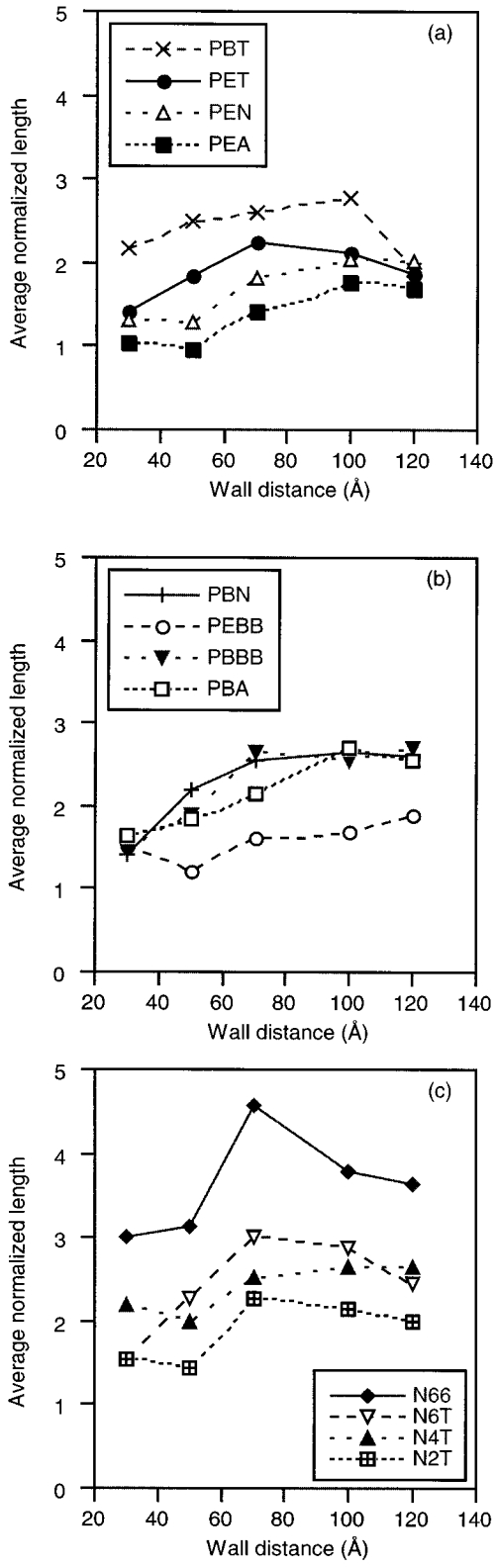

Figure 11. Average normalized bridge length ((contour length of bridge)/(wall spacing)) at equilibrium, as a function of intercrystalline wall distance for various polymers: (a and b) polyesters; (c) polyamides (system after 100 000 interchange reactions from an *initial system with no bridges*; averaged over 10 simulation runs).

of chains. An issue that can arise in this regard pertains to whether it would alter significantly the steady-state result. Indeed, several models for morphology of semicrystalline polymers have predicted dense structures, with significant order, at crystal interface regions.[43−48] It is also widely accepted that even noncrystalline polymers contain significant local order.[49] However, it should also be noted here that models for polymer domains that ignore such considerations have been still remarkably successful in predicting their properties, in "amorphous" as well as semicrystalline polymers, especially at temperatures well above T_g.[50−53] Also, oriented polymers of similar densities, but substantially different intrinsic rigidities, retain their crystalline orientation but otherwise reach significantly different morphology and properties with SSP.[16,20,54] It shows clearly the dominant effect of chain partition functions in this close-to-melting process. There is also clear evidence, in the work of Lenz et al., that the presumably dense interface with the crystal is accessible for interchange reactions to a significant extent.[55,56] If the functional sites that are next to crystal surfaces are accessible for interchange reactions, the consequent interchange of monomer units at its interface can facilitate the growth of a crystal of one type of monomer units in a random copolymer. A simultaneous outcome of this process would be the creation of block sequences of the crystallizable monomer units in an initially random copolymer.[55,56]

The thermorheological responses (thermal shrinkage, thermal stress) of oriented fibers and films show clearly that conformation-dictated free energies, and not space-filling issues, dictate to a large extent the equilibrium sought by chains in the noncrystalline domains. Also, crystallization-induced morphological changes in the noncrystalline regions in oriented fibers, the morphology and properties of filaments of segmented elastomers with oriented crystalline morphologies, etc., also show that space-filling considerations might arise only as a refinement and not as an issue of primary concern.

A simple example of direct relevance to the current work is the dramatically different consequences of interchange reactions in fibers of drawn semirigid polymers (e.g., nylon 66 and PET) and extruded rodlike polymers, e.g., poly(*p*-phenylene terephthalamide), both of which are dense structures and initially of comparable mechanical properties. While the equilibrium sought by nylon 66 or PET leads to a substantial reduction in modulus and strength, the PPTA filament exhibits an equally substantial increase in the same. The reduction of properties of the relatively flexible polymers occurs despite an order of magnitude increase in molecular weight. It is due to the fact that the equilibrium spatial pathways of chains in the noncrystalline phase are dictated *not* by any significant tendency to reflect the order present in the still oriented crystals but by their pronounced tendency to transform bridging chains into loops, a process dictated by the free energies of chains.

It is most important to recognize the fact that the topological changes which result from interchange reactions *do not require large-scale motions of chains*. Space filling constraints are of only secondary concern in this case because these reactions can—and do—occur with facility, to the extent that polymerization in the solid state can be quantitatively described by interchange-assisted kinetics, without any consideration of space-filling issues.[15]

The recognition that the chains in the interphase are likely to have the imprint of the crystal structure is the reason that the first three bonds of the chains have been restricted to be in the same conformational sequence as that in the crystal. However, the refinements that

can be made by considering packing-related issues, especially with regard to the *progression toward dynamic equilibrium*, cannot be discounted. For this purpose, it would be necessary to maintain a record of coordinate positions of all the sites for interchange reactions, with the choice of reaction of an end group restricted to be with those in its neighborhood. The relative probabilities of reactions among the accessible sites would be still dictated by the partition functions of the different outcomes, as formulated in the present study.

Summary and Conclusions

The rate-limiting step in many SSP processes is the removal of the condensate molecule, whose reaction can negate the effect of the polymerization step.[57−59] By carrying out SSP in thin structures, such as fibers and thin films, the reverse reaction can be minimized and high molecular weights can be obtained on a practically desirable time scale.[15] In any case, the mechanism that *facilitates* SSP in polymers, such as polyesters and polyamides, is "chemical" diffusion of the functional groups, caused by the interchange reactions, such as alcohol−ester or amine−amide.[15] An important implication of the interchange-dictated mechanism of SSP is that they have the potential to cause substantial changes in the intercrystalline *morphology* of homopolymers as well as copolymers. Since these reactions leave the composition of chemical functional groups unchanged, their consequences in homopolymers consist entirely of changes in the distribution of lengths and topology of the chains (bridge, loop, anchor chain or free chain) produced. In this regard, the relative probabilities of interchange reactions, e.g., between a functional end and the functional links in its neighborhood, would be dictated by relative thermodynamic preferences for the different topological outcomes of these reactions. The following are the essential elements of the framework that has been formulated to model this process.

•The noncrystalline domain in a uniaxially oriented polymer is modeled as the domain between two infinite parallel walls. However, if necessary, the methods developed here can be easily extended to impose other physical boundaries.

•The different chains are characterized by the combination of their type, length and the domain in which they are restricted to lie.

•Loops and bridges are characterized only by the face(s) on which they are anchored and the distance between the two confining boundaries. While their lateral coordinates have been implicitly included in the Monte Carlo analysis, their effect has not been considered or recorded explicitly.

•The relative rates of reactions with different topological outcomes are postulated to be governed by the ratios of the partition functions of those outcomes.

The partition function of a chain of a particular topological type and length has been determined through a novel scaling from RIS−Monte Carlo simulations.

The results and analysis reveal the following.

•The molecular-level morphology of the noncrystalline phase evolves, through interchange reactions, toward a dynamic equilibrium during post-extrusion solid-state polymerization. This equilibrium governs the relative concentrations, and the distribution of lengths, of the topologically different chains in the noncrystalline phase. The framework developed here has been shown to be robust, with the same dynamic equilibrium distributions resulting from vastly different initial conditions.

•Two distinct aspects of reactions during SSP can act together, or compete, to either enhance or diminish the mechanical properties. If increase in molecular weight occurs without adverse morphological changes, it would produce higher mechanical performance.[12] However, the present work shows that interchange reactions during SSP would also change the relative concentrations of different topological chains in the intercrystalline region. If SSP is carried out in the post-drawing stage, it is likely that, with most semiflexible polymers, the initial concentration of bridging chains would be higher than the equilibrium concentration, and so interchange reactions would tend to decrease the bridge content. In such cases, SSP can be expected to produce adverse consequences vis-a-vis mechanical properties. On the other hand, with polymers of relatively high intrinsic rigidity, SSP can produce a desired increase in bridge content, along with narrowing of the distribution of length of bridging chains.

•The framework formulated here would allow a large number of *gedanken* experiments to identify polymers whose thermodynamic equilibrium structures might result in a better *combination of high strength and toughness* than those which have been achieved from the flexible or the rodlike polymers.

•The methodology described here can also be used to determine equilibrium distributions of chain structures in oriented polymers, even if they do not offer the required functionalities for interchange reactions. Fictitious sites for interchange reactions can be introduced along the chains of any polymer and reactions at different sites can be modeled in the same manner as described here, with the relative probabilities of reactions at different sites dictated again by the partition functions of the chains produced.

Nomenclature

l, length of a chain in the intercrystalline domain, expressed as number of repeat units

l_{av}, average length of a chain in the intercrystalline domain

$\underline{\bar{h}}$, intercrystalline wall distance (m)

$Q_L\{l,\underline{\bar{h}}\}$, partition function of a loop of contour length l, confined between two parallel walls that are separated by a distance $\underline{\bar{h}}$

$Q_B\{l,\underline{\bar{h}}\}$, partition function of a bridging chain of contour length l, confined between two parallel walls that are separated by a distance $\underline{\bar{h}}$

$Q_{AC}\{l,\underline{\bar{h}}\}$, partition function of an anchor chain of contour length l, confined between two parallel walls that are separated by a distance $\underline{\bar{h}}$

$Q\{l\}$, partition function of an *unconfined* chain of contour length l

$N_B\{l,\underline{\bar{h}}\}$, number of accepted bridging chains, out of a total of $N\{l\}$ simulated chains, with intercrystalline wall distance $\underline{\bar{h}}$ and contour length l

$N_L\{l,\underline{\bar{h}}\}$, number of accepted loops, out of a total of $N\{l\}$ simulated chains, with intercrystalline wall distance, $\underline{\bar{h}}$ and contour length, l

$N_{AC}\{l,\underline{\bar{h}}\}$, number of accepted anchor chains, out of a total of $N\{l\}$ simulated chains, with intercrystalline wall distance, $\underline{\bar{h}}$ and contour length, l

$P_B(\bar{l}_i)$, fraction of chains in the intercrystalline domain that are bridging chains of normalized contour length, $\bar{l}_i$

$P_L(\bar{l}_i)$, fraction of chains in the intercrystalline domain that are loops of *normalized* contour length, $\bar{l}_i$ (See eq 16)
L_R, extended length of a repeat unit
Q, partition function
$\{Q_i(\bar{l}_i,\bar{h})\}$, set of partition functions of all the chains in a noncrystalline domain
$G\{\bar{h}\}$, free energy of a noncrystalline domain
$N\{\bar{l}\}$ (or) N_T, total number of chains generated (accepted and rejected), with contour length = l, in Monte Carlo simulation of the chains in the intercrystalline domain
m_{RU}, molar mass of a repeat unit (kg/mol)
n, total number of chains in the intercrystalline domain
N_A, Avogadro's number
ρ, density of the intercrystalline domains (kg/m^3)

References and Notes

(1) Popli, R.; Roylance, D. *Polym. Eng. Sci.* **1985**, *25*, 828.
(2) Yegorov, Y. A.; Zhizhenkov, V. V.; Marikhin, V. A.; Myasnikova, L. P.; Popov, A. *Polym. Sci. USSR* **1983**, *25*, 805.
(3) Lustiger, A.; Ishikawa, N. *J. Polym. Sci., Polym. Phys. Ed.* **1991**, *29*, 1047.
(4) Varyukhin, S. E.; Zaitsev, M. G. *Polymer* **1990**, *31*, 1750.
(5) Zaitsev, M. G.; Varyukhin, S. Y. *Intern. J. Polym. Mater.* **1993**, *22*, 33.
(6) Zaitsev, M. G.; Varyukhin, S. Y. *Polym. Sci. USSR* **1990**, *32*, 977.
(7) Varyukhin, S. Y.; Zaitsev, M. G. *Polym. Sci. USSR* **1989**, *31*, 2042.
(8) Itoyama, K. *J. Polym. Sci., Polym. Phys. Ed.* **1981**, *19*, 1873.
(9) Guttman, C. M.; DiMarzio, E. A. *Macromolecules* **1982**, *15*, 525.
(10) Leermakers, F. A. M.; Scheutjens, J. M. H. M.; Gaylord, R. J. *Polymer* **1984**, *25*, 1577.
(11) Mansfield, M. L. *J. Phys. Chem.* **1989**, *93*, 6926.
(12) Yoon, H. N. *Colloid Polym. Sci.* **1990**, *268*, 230.
(13) Pakhomov, P. M.; Yegorov, Y. A.; Zhizhenkov, V. V.; Chegolya, A. S. *Polym. Sci. USSR* **1991**, *32*, 137.
(14) Zaitsev, M. G.; Stremyakov, S. A.; Yegorov, Y. A. Z. V. V.; Razumovskaya, I. V. *Polym. Sci. USSR* **1986**, *28*, 226.
(15) Almonacil, C.; Srinivasan, R.; Narayan, S.; Desai, P.; Abhiraman, A. S. *Macromolecules* **1998**, *31*, 6813.
(16) Srinivasan, R. Ph.D. Thesis, Georgia Institute of Technology, Atlanta, GA, 1994.
(17) Miyagi, A.; Wunderlich. B. *J. Polym. Sci., Polym. Phys. Ed.* **1972**, *10*, 2073.
(18) Miyagi, A.; Wunderlich, B. *J. Polym. Sci., Polym. Phys. Ed.* **1972**, *10*, 2085.
(19) Kyotsukuri, T.; Tada, Y. *Sen'i Gakkaishi* **1980**, *36*, 157.
(20) Narayan, S. M.S. Thesis, Georgia Institute of Technology, Atlanta, GA, 1995.
(21) Jager, J.; Juijn, J. A.; Van Den Heuvel, C. J. M.; Huijts, R. A. *J. Appl. Polym. Sci.* **1995**, *57*, 1429.
(22) Yamanobe, T.; Matsuda, H.; Imai, K.; Hirata, A.; Mori, S.; Komoto, T. *Polym. J.* **1996**, *28*, 177.
(23) Yoon, K. H.; Lee, S. C.; Park, O. O. *Polym. Eng. Sci.* **1995**, *35*, 1807.
(24) Yoon, K. H.; Lee, S. C.; Park, O. O. *Polym. J.* **1994**, *26*, 816.
(25) Shashoua, V. E.; Eareckson, W. M. *J. Polym. Sci.* **1959**, *40*, 343.
(26) Gaymans, R. J. *J. Polym. Sci., Polym. Chem. Ed.* **1985**, *23*, 1599.
(27) Frazer, A. H.; Anderson, B. C.; Fukunaga, T. *J. Polym. Sci., Polym. Chem. Ed.* **1985**, *23*, 2791.
(28) Watanabe, J.; Hayashi, M. *Macromolecules* **1989**, *22*, 4083.
(29) Watanabe, J.; Hayashi, M. *Macromolecules* **1995**, *28*, 2073.
(30) Carr, P. L.; Nicholson, T. M.; Ward, I. M. *Polym. Adv. Technol.* **1997**, *8*, 592.
(31) Binder, K.; Ed. *Monte Carlo and Molecular Dynamics Simulations in Polymer Science*; Oxford University Press: New York, 1995.
(32) Montaudo, M. S. *Macromolecules* **1993**, *26*, 2451.
(33) Jo, W. H.; Lee, J. W.; Lee, M. S.; Kim, C. Y. *J. Polym. Sci., Polym. Phys. Ed.* **1996**, *34*, 725.
(34) Jang, S. S.; Ha, W. S.; Jo, W. H.; Youk, J. H.; Kim, J. H.; Park, C. R. *J. Polym. Sci., Polym. Phys. Ed.* **1998**, *36*, 1637.
(35) Mattice, W. L.; Suter, U. W. In *Conformational Theory of Large Molecules*; Wiley: New York, 1994; p 137.
(36) Flory, P. J. *Macromolecules* **1974**, *7*, 381.
(37) Flory, P. J.; Williams, A. D. *J. Polym. Sci., Polym. Chem. Ed.* **1967**, *5*, 399.
(38) Williams, A. D.; Flory, P. J. *J. Polym. Sci., Polym. Phys. Ed.* **1967**, *5*, 417.
(39) Bahar, I.; Mattice, W. L. *J. Chem. Phys.* **1989**, *11*, 6783.
(40) *Polymer User Guide*; Molecular Simulations: San Diego, CA, 1998.
(41) Guttman, C. M.; DiMarzio, E. A.; Hoffman, J. D. *Polymer* **1981**, *22*, 1466.
(42) Almonacil, C. Ph.D. Thesis, Georgia Institute of Technology, Atlanta, GA, 1998.
(43) Flory, P. J.; Yoon, D. Y.; Dill, K. A. *Macromolecules* **1984**, *17*, 862.
(44) Marqusee, J. A.; Dill, K. A. *Macromolecules* **1986**, *19*, 2420.
(45) Marqusee, J. A.; Dill, K. A. *Macromolecules* **1989**, *22*, 472.
(46) Termonia, Y. *Macromolecules* **1995**, *28*, 7667.
(47) Kumar, S. K.; Yoon, D. Y. *Macromolecules* **1989**, *22*, 3458.
(48) Kumar, S. K. Yoon, D. Y. *Macromolecules* **1991**, *24*, 5414.
(49) Keinath, S. E.; Miller, R. L.; Rieke, J. K. Eds. *Order in the Amorphous "State" of Polymers*; Plenum Press: New York, 1985.
(50) Davis, H. A. A Theoretical Basis for the Physical Behavior of Synthetic Fibers. In *Advances in Fiber Science*; Mukhopadhyay, S. K., Ed.; The Textile Institute (Pub): Manchester, U.K., 1992; pp 141−180.
(51) Davis, H. A. *J. Text. Inst.* **1995**, *86*, 332.
(52) Nanavati, H.; Desai, P.; Abhiraman, A. S. *Comput. Theor. Polym. Sci.* **1999**, *9*, 165.
(53) Meissner, B. *Polymer* **2000**, *21*, 7827.
(54) Fitzgerald, J. A.; Irwin, R. S.; Memeger, W. *Macromolecules* **1991**, *24*, 3291.
(55) Lenz, R. W.; Schuler, A. N. *J. Polym. Sci., Polym. Symp.* **1978**, *63*, 343.
(56) Lenz, R. W.; Jin, J. I.; Schuler, A. N. *Polymer* **1984**, *24*, 327.
(57) Chen, F. G.; Griskey, R. G.; Beyer, G. H. *AIChE J.* **1969**, *15*, 680.
(58) Mallon, F. K.; Ray, W. H. *J. Appl. Polym. Sci.* **1998**, *69*, 1233.
(59) Mallon, F. K.; Ray, W. H. *J. Appl. Polym. Sci.* **1998**, *69*, 1775.

MA9920339